VOLUME ANALYSIS AND VOID-FREE DESIGN OF THE WORKSPACE OF A 7-DOF MANIPULATOR

Xinglei ZHANG[1 *], Yu XU[1], Su XU[2], Chao HAN[1], Guocheng LIU[3], Xiaodong LUO[4]

When the size of the connecting rod in a 7-DOF manipulator changes to a certain extent, the workspace obtained using the Monte Carlo method cannot easily reveal changes, which is not conducive to optimizing the connecting rod parameters. An algorithm for calculating the workspace volume, based on the principles of three-dimensional functional calculus, is proposed. To avoid voids in the workspace of the 7-DOF manipulator and to affect its motion performance, a void-free constraint for the workspace is derived. The algorithm for calculating the workspace volume and the void-free constraint are simulated and verified using the 7-DOF manipulator.

Key words: 7-DOF manipulator, workspace volume, void-free design.

1. Introduction

The workspace is an important kinematic indicator for measuring the working performance of a 7-DOF manipulator [1]. The solution methods include analytical methods [2] and numerical methods, etc. Numerical methods are the primary means for obtaining the workspace. By calculating the boundary surface of the workspace through forward kinematics, one can observe the motion range of the manipulator in various coordinate directions. The Monte Carlo method is one of the most commonly used numerical methods [3].

The mapping of each joint variable of a 7-DOF manipulator to the position and orientation description of the end-effector in Cartesian coordinates is more complex. The joint positions of the Monte Carlo method follow a uniform distribution within its range, and after mapping from joint space to operating space, their spatial point distribution becomes non-uniform [4]. This results in low boundary accuracy when obtaining the workspace of a 7-DOF manipulator using the Monte Carlo method. Furthermore, when the size of the connecting rod changes to a certain extent, it is not easy to discern whether the workspace

[1]School of Mechanical Engineering, Jiangsu Ocean University, Lianyungang, 222005, China.
[2]School of Innovation and Entrepreneurship, Jiangsu Ocean University, Lianyungang, 222005, China.
[3]Weifang Zhongying Chemical limited liability company, Weifang, 261021, China.
[4]Panzhihua Steel City Group Co., Ltd. Cold Cooperative Branch, Panzhihua, 617023, China.
*Email: zhangxingfulove@163.com

obtained by the Monte Carlo method has changed, which is not conducive to the optimization of the connecting rod parameters when the workspace is used as the objective function.

Rutong Dou [5] improved the display accuracy of the working space by employing a decimation Monte Carlo method. Zhiyuan Zhao [6] proposed an improved Monte Carlo method based on the normal distribution, which enhanced the solution accuracy of the working space by setting a precision threshold. SR Pundru [7] obtained the workspace of a multi-position manipulator using least square and Renka Cline gridding approaches. Peidro [8] sought the boundary points of the workspace, and then sampled them near the joint positions of the boundary points through a Gaussian distribution, bringing the sampling values into its forward kinematics equation, which improved the distribution density of workspace points at the boundary. Zhizhong Liu [9] layered the workspace and searched for boundary points at each layer, then added random points at each layer's boundary points to generate clear workspace boundaries. The above scholars only made improvements based on the Monte Carlo method. Although they improved the solution accuracy of the workspace, they did not solve the difficulty of not being able to easily detect whether the workspace had changed when the connecting rod size changed to a certain extent. Therefore, Zhenbang Xu [10] used a volume element algorithm to calculate workspace volume based on the Monte Carlo method, and refined the boundary region, which improved the accuracy of workspace volume calculation. Hongbo Liu [11] used the Monte Carlo method to obtain a point cloud map of the workspace and processed the boundary point cloud using the convex hull function in MATLAB to generate an envelope space. The volume of the envelope space was calculated and approximated as the volume of the workspace. Although the aforementioned scholars have improved the accuracy of the workspace obtained by the Monte Carlo method through some approaches, the workspace is difficult to describe mathematically, which is not conducive to the optimization of link parameters when the working space is used as the objective function.

The presence of voids in the workspace can reduce the motion performance of a 7-DOF manipulator, which is caused by an unreasonable combination of connecting rod sizes. Zhaohui Lan [12] analyzed the conditions for the disappearance of voids in the workspace of parallel manipulators and conducted case analyses. However, the analysis of voids in the workspace of serial robots is almost a blank slate. Given that the presence of voids will reduce the accuracy of the Monte Carlo method in solving the workspace of a 7-DOF manipulator, further affecting the optimization of its linkage parameters. Therefore, how to obtain a high-precision algorithm for calculating the workspace volume of a 7-DOF manipulator and derive a void-free design condition for the workspace are the issues that need to be addressed in this paper.

2. Research on workspace volume of a 7-DOF manipulator

2.1 Analysis of the workspace of a 7-DOF manipulator

In this paper, a 7-DOF manipulator designed in our laboratory is taken as an example for workspace analysis. The 3D model of the manipulator is shown in Figure 1 (a). The spatial coordinate system for the 7-DOF manipulator is constructed and depicted in Figure 1 (b). The modified D-H parameters are shown in Table 1. The Monte Carlo method, one of the most commonly used numerical methods for solving the workspace of robotic manipulators, is employed for the manipulator's workspace analysis.

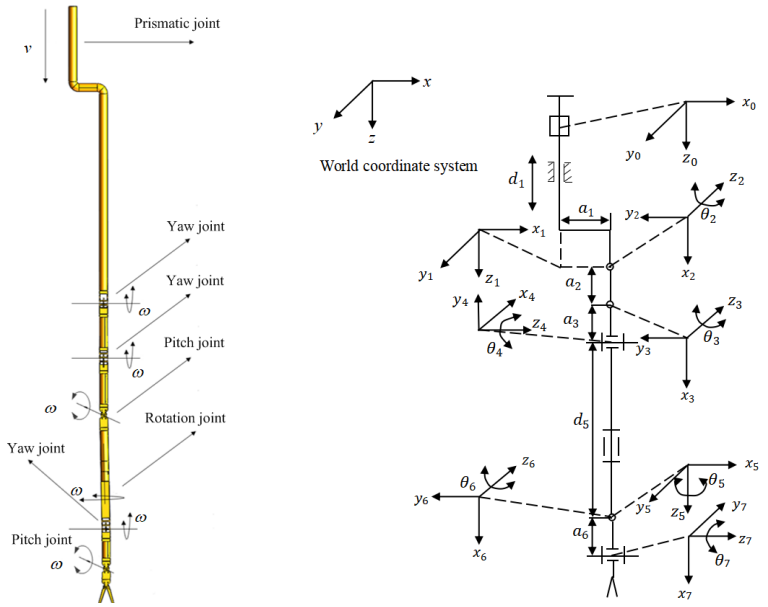

(a) The 3D model (b) The spatial coordinate system

Fig. 1. The 3D model and coordinate system of the 7-DOF manipulator

Table 1

The modified D-H parameters of the 7-DOF redundant manipulator

i	α_{i-1} (rad)	a_{i-1} (mm)	d_i (mm)	θ_i (rad)
1	0	0	d_1	0
2	$\pi/2$	a_1	0	θ_2 ($\pi/2$)
3	0	a_2	0	θ_3 (0)
4	$\pi/2$	a_3	0	θ_4 ($\pi/2$)
5	$\pi/2$	0	d_5	θ_5 ($\pi/2$)
6	$\pi/2$	0	0	θ_6 ($\pi/2$)
7	$\pi/2$	a_6	0	θ_7 (0)

Two sets of connecting rod sizes are considered, in the first set: $a_1 = 20\text{mm}$, $a_2 = a_3 = 50\text{mm}$, $d_5 = 100\text{mm}$, and $a_6 = 30\text{mm}$, in the second set : $a_1 = 20\text{mm}$, $a_2 = 60\text{mm}$, $a_3 = 40\text{mm}$, $d_5 = 105\text{mm}$, and $a_6 = 25\text{mm}$. When using the Monte Carlo method to determine the workspace, we aimed to explore the appropriate number of joint position divisions to ensure that there is no guarantee the method will not generate false voids. We conducted the following tests using the first set of dimensions, dividing the range of joint positions into 30,000 and 200,000 segments to obtain the corresponding workspace cloud maps. We then vertically stratified these two cloud maps along the *x*, *y*, and *z* axes by 50mm and 20mm, respectively (with this paper selecting three stratification planes in each axial direction) to observe the display effect of the cloud map position points, as shown in Figures 2 and 3. It is found that the former workspace cloud map has an uneven distribution of position points, with large gaps between many points, which may be considered as "voids" (voids generally being circular or elliptical in shape). In contrast, the latter workspace cloud map showed a more uniform distribution of position points with smaller gaps, facilitating the easier identification of any actual voids.

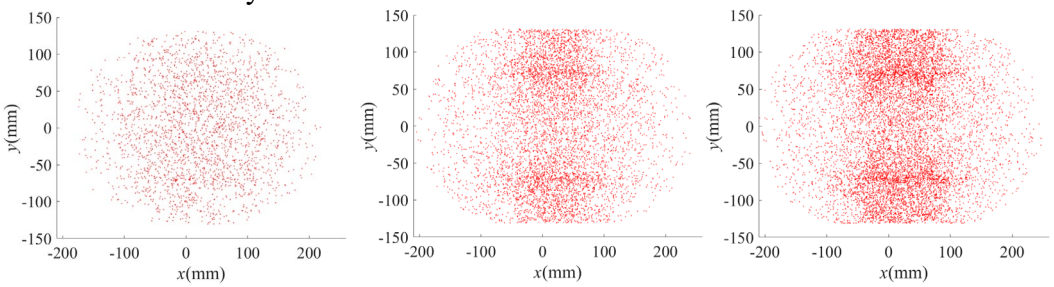

(a) *x-o-y* ($z \in [-150, -100]\text{mm}$) (b) *x-o-y* ($z \in [-100, -50]\text{mm}$) (c) *x-o-y* ($z \in [-50, 0]\text{mm}$)

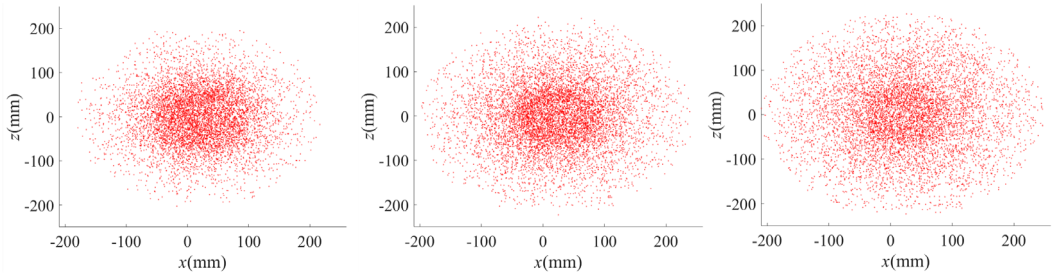

(d) *x-o-z* ($y \in [-130, -80]\text{mm}$) (e) *x-o-z* ($y \in [-80, -30]\text{mm}$) (f) *x-o-z* ($y \in [-30, 20]\text{mm}$)

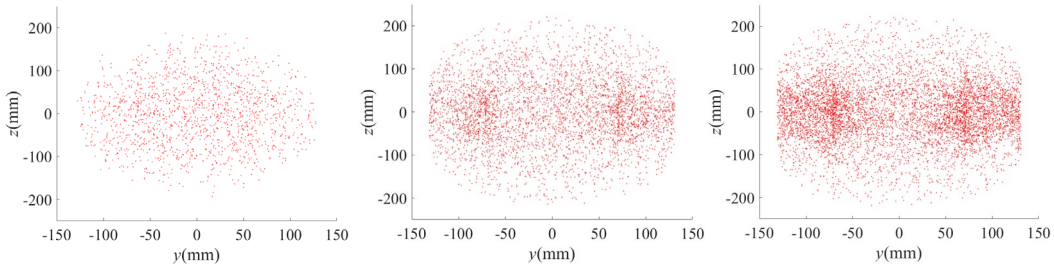

(g) *y-o-z* ($x \in [-150, -100]$mm) (h) *y-o-z* ($x \in [-100, -50]$mm) (i) *y-o-z* ($x \in [-50, 0]$mm)

Fig. 2. The workspace cloud map corresponding to the division of each joint into 30,000 segments.

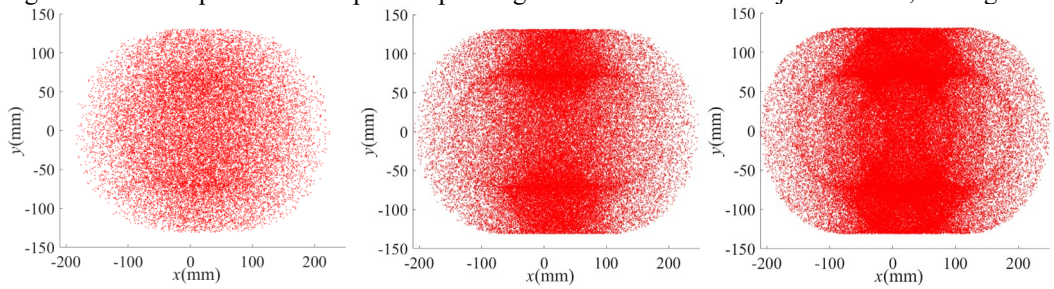

(a) *x-o-y* ($z \in [-100, -80]$mm) (b) *x-o-y* ($z \in [-80, -60]$mm) (c) *x-o-y* ($z \in [-60, -40]$mm)

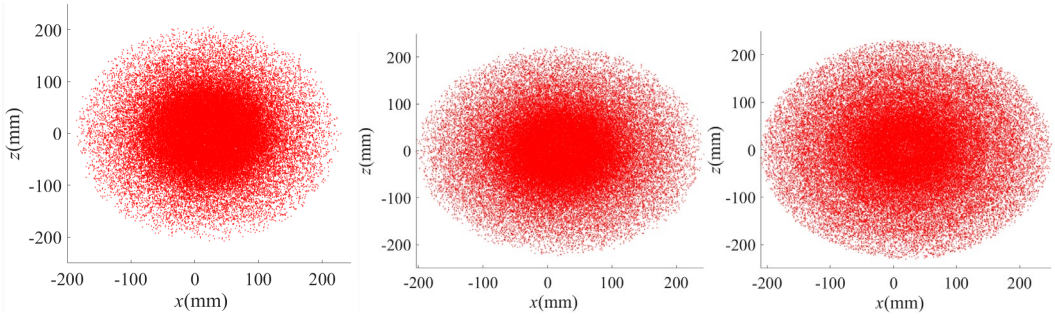

(d) *x-o-z* ($y \in [-100, -80]$mm) (e) *x-o-z* ($y \in [-80, -60]$mm) (f) *x-o-z* ($y \in [-60, -40]$mm)

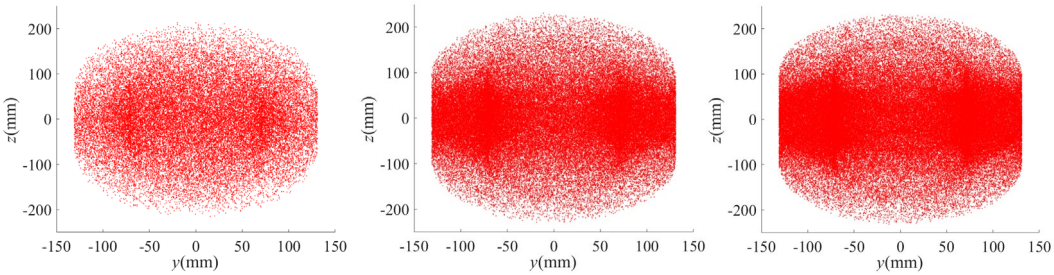

(g) *y-o-z* ($x \in [-100, -80]$mm) (h) *y-o-z* ($x \in [-80, -60]$mm) (i) *y-o-z* ($x \in [-60, -40]$mm)

Fig. 3. The workspace cloud map corresponding to the division of each joint into 200,000 segments.

Therefore, this study divides the joint variables of each joint into 200,000 segments and obtains a workspace cloud map corresponding to the sizes of the two sets of connecting rods mentioned above, as shown in Figures 4 and 5. It is difficult to distinguish the differences in the reachable areas of the two

workspaces. Therefore, using the workspace as the objective function is not conducive to the optimization of the connecting rod parameters.

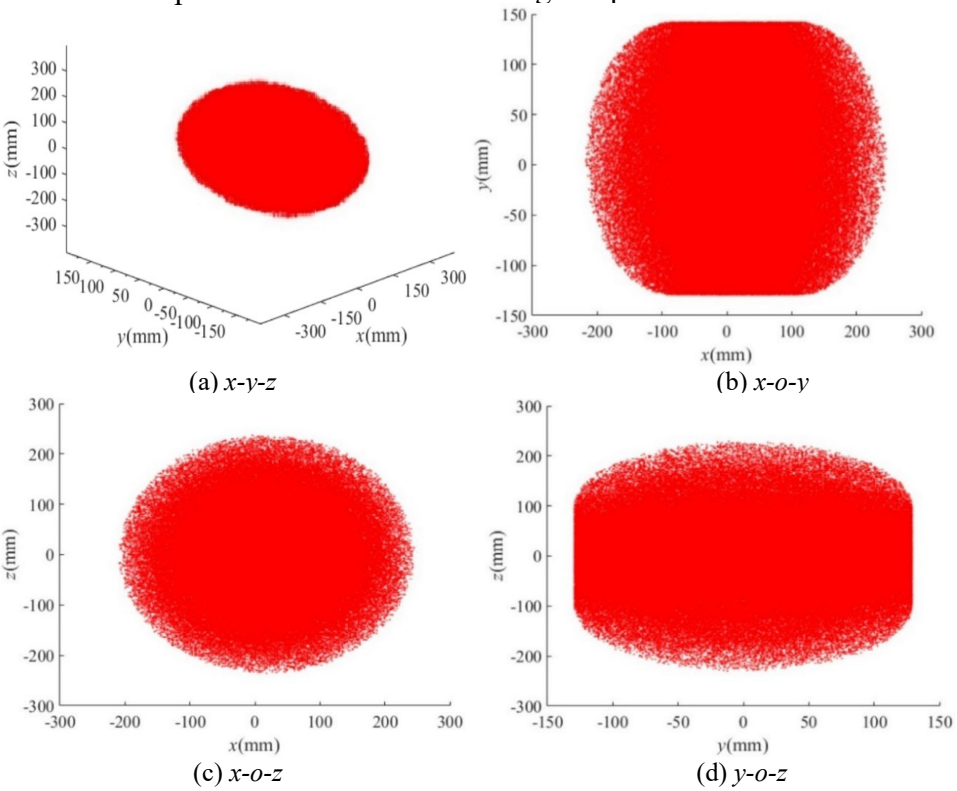

(a) *x-y-z* (b) *x-o-y*

(c) *x-o-z* (d) *y-o-z*

Fig. 4. Contours of the 7-DOF manipulator workspace corresponding to the first set of connecting rod

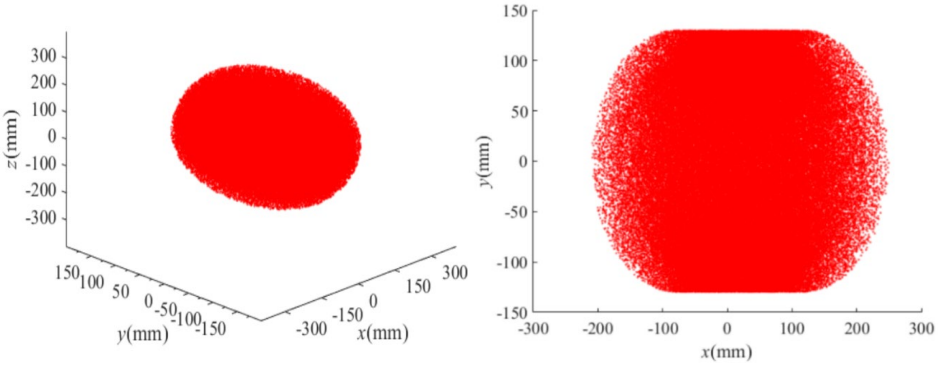

(a) *x-y-z* (b) *x-o-y*

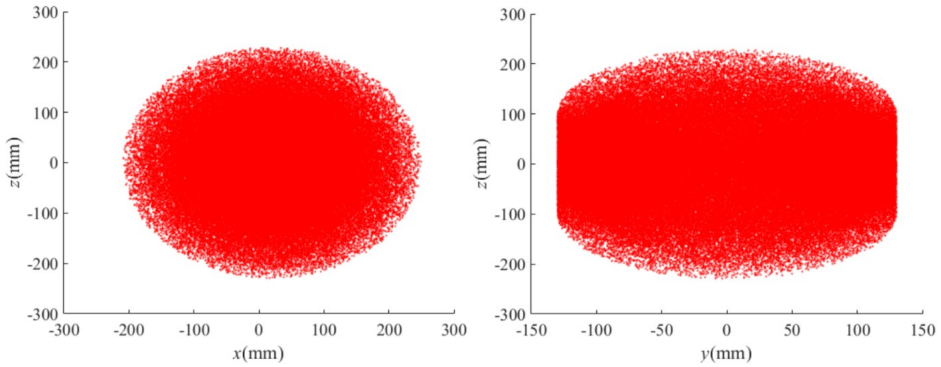

(c) *x*-*o*-*z* (d) *y*-*o*-*z*

Fig. 5. Contours of the 7-DOF manipulator workspace correspond to the second set of connecting rod

2.2 Design of Algorithm for Solving the Volume of the workspace of a 7-DOF manipulator

To address the difficulty of using the workspace obtained by the Monte Carlo method as an objective function, which is not conducive to optimizing the parameters of connecting rods. A solution algorithm for the workspace volume of a 7-DOF manipulator based on the principles of three-dimensional function calculus is proposed. The steps for establishing the mathematical model are as follows:

(1) A sufficiently clear cloud contour of a 7-DOF manipulator workspace is obtained through the Monte Carlo method, and the minimum value x_1 and maximum value x_2 in the *x*-axis direction are found. The workspace is divided in L layers perpendicular to the *x*-axis direction, with a thickness of $h = \frac{x_2 - x_1}{L}$ for each layer, as shown in Figure 6 (a).

(2) In step (1), each slice is approximately regarded as a thin three-dimensional body of different shapes parallel to the *y*-*o*-*z* plane. The minimum value $y_{\min}$ and maximum value $y_{\max}$ of each thin three-dimensional body in the *y*-axis direction are found, and then divided into rectangles with M columns, as shown in Figure 6 (b). Each column of rectangles is further divided into H layers along the *z*-axis, producing H+1 *z*-coordinate values, which are then sorted in ascending order, with $z_1 < z_2 < \cdots z_{\tilde{i}} < z_{\tilde{i}+1} < \cdots z_{H+1}$. Eq. (1) can be used to determine whether there is an intermediate void in the workspace of manipulator, as shown in Figure 6 (c). If Eq. (1) is satisfied, it indicates that there is no void in the workspace; otherwise, there is a void.

$$z_{\tilde{i}+1} - z_{\tilde{i}} \le \kappa \tag{1}$$

Where κ is associated with the transverse dimension of the designed robotic manipulator's connecting rod (If the rod is cylindrical, the value of κ is

related to the rod's diameter (d), and it can be taken as $\kappa = (0.6 \sim 0.9)d$). If the void size is less than the transverse dimension of the connecting rod, the impact on the robotic manipulator's performance is relatively minor; conversely, the opposite holds true.

The area of layer $\tilde{i}$ in each thin three-dimensional body can be calculated using Eqs. (2) to (4):

$$s(\tilde{i}) = f(\tilde{i}) - g(\tilde{i}) \tag{2}$$

$$f(\tilde{i}) = \kappa(z_{\max}^{\tilde{i}} - z_{\min}^{\tilde{i}}) \tag{3}$$

$$g(\tilde{i}) = \begin{cases} \kappa(z_{\tilde{i}+1} - z_{\tilde{i}}) & z_{\tilde{i}+1} - z_{\tilde{i}} > \kappa \\ 0 & z_{\tilde{i}+1} - z_{\tilde{i}} \le \kappa \end{cases} \tag{4}$$

Therefore, the total area of each thin three-dimensional body is shown in Eq. (5):

$$S(j) = \sum_{\tilde{i}=1}^{M} s(\tilde{i}) \tag{5}$$

(3) The volume of the jth layer of thin three-dimensional volume perpendicular to the x-axis direction is obtained from Eq. (6), and the workspace volume of a 7-DOF manipulator is calculated using Eq. (7):

$$v(j) = S(j)\frac{x_2 - x_1}{L} \tag{6}$$

$$V = \sum_{j=1}^{L} v(j) \tag{7}$$

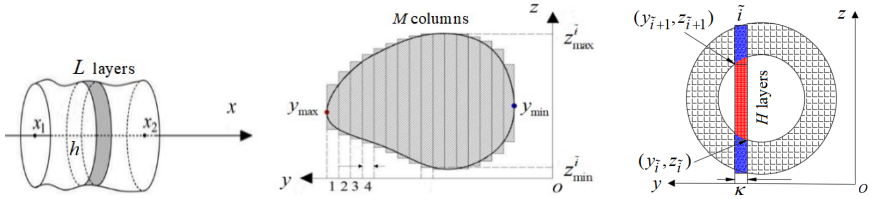

(a) Workspace segmentation (b) Plane segmentation (c) The void of the workspace

Fig. 6. Schematic diagram of workspace volume algorithm

Based on the two sets of workspace cloud maps obtained above, $L = 30$ and $M = 20$ are set. The corresponding workspace volumes are calculated through the proposed workspace volume algorithm: $V_{\text{first}} = 4.5 \times 10^7\ \text{mm}^3$, $V_{\text{second}} = 4.7 \times 10^7\ \text{mm}^3$. When there is a certain change in the size of the connecting rod, the volume difference calculated by the proposed algorithm is significant, which can intuitively reflect the change in the workspace. This provides theoretical support for optimizing connecting rod parameters using workspace volume as the objective function in the future.

3. No void design in workspace of a 7-DOF manipulator

The presence of voids in the workspace of a 7-DOF manipulator can reduce the motion area of the end effector, affecting its motion performance. To better optimize the linkage parameters, it is necessary to design a void free workspace for the 7-DOF manipulator. Neglecting the influence of joint accuracy and control system accuracy on the workspace of the 7-DOF manipulator, and considering that voids caused by setting joint position constraints due to the needs of the working environment cannot be avoided. This section derives the constraint conditions for a workspace without joint position constraints.

Based on Figure 1, the schematic diagrams are made as shown in Figure 7 for analysis. O_0 is the origin of the base coordinate system. O_4 and O_6 are the rotation points of the fourth and sixth joints, respectively. O_7 and $O_7^{'}$ are the two points when connecting rod 6 rotates around O_6 to be collinear with segment O_4O_6, respectively. When the seventh joint's rotation point is at position O_7, if $|a_2 + a_3| < |d_5 - a_6|$, a black circular void will appear as shown in Figure 7 (a). At this point, to ensure that there are no voids in the workspace, Eq. (8) needs to be satisfied:

$$|a_2 + a_3| \geq |d_5 - a_6| \tag{8}$$

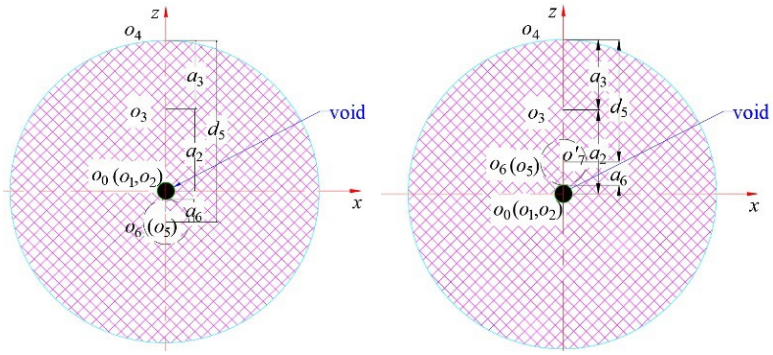

Fig. 7 Workspace void analysis configuration of the 7-DOF manipulator

Similarly, when the seventh joint's rotation point is at position $O_7^{'}$, if $|a_2 + a_3| > |d_5 + a_6|$, a black circular void will also appear in the workspace as shown in Figure 7 (b). At this point, to ensure that there are no voids in the workspace, it is also necessary to satisfy Eq. (9):

$$|a_2 + a_3| \leq |d_5 + a_6| \tag{9}$$

Therefore, to ensure that there are no voids in the workspace, Eq. (10) needs to be satisfied:

$$|d_5 - a_6| \leq |a_2 + a_3| \leq |d_5 + a_6| \tag{10}$$

By analogy, the design condition for a void-free workspace of another 7-DOF manipulator can be derived. This condition provides a rational match between the sizes of the connecting rods during the manipulator structure design to prevent the generation of voids in the workspace.

4. Validity verification of the design with no voids in the workspace of the 7-DOF manipulator

To verify the effectiveness of the 7-DOF manipulator workspace without void constraints, three sets of connecting rod sizes were established and compared for analysis. Group 1: $a_1 = 20\text{mm}$, $a_2 = 40\text{mm}$, $a_3 = 50\text{mm}$, $d_5 = 120\text{mm}$, $a_6 = 20\text{mm}$ does not satisfy Eq. (8). Group 2: $a_1 = 20\text{mm}$, $a_2 = a_3 = 70\text{mm}$, $d_5 = 60\text{mm}$, $a_6 = 20\text{mm}$, does not satisfy Eq. (8). Group 3: $a_1 = 20\text{mm}$, $a_2 = 60\text{mm}$, $a_3 = 50\text{mm}$, $d_5 = 100\text{mm}$, $a_6 = 30\text{mm}$, satisfies Eq. (8). The workspace cloud point maps of the robotic arm using the Monte Carlo method are obtained. Among them, the workspace corresponding to the dimensions of the first group of connecting rods is shown in Figure 8. The voids in the workspace are searched along the *x*, *y*, and *z* directions with a thickness of 10mm for each layer. It is found that the first group of connecting rods had a void with a diameter of about 20mm in the *x-o-z* plane and within $y \in [-25, 25]\text{mm}$, as shown in Figure 8 (c).

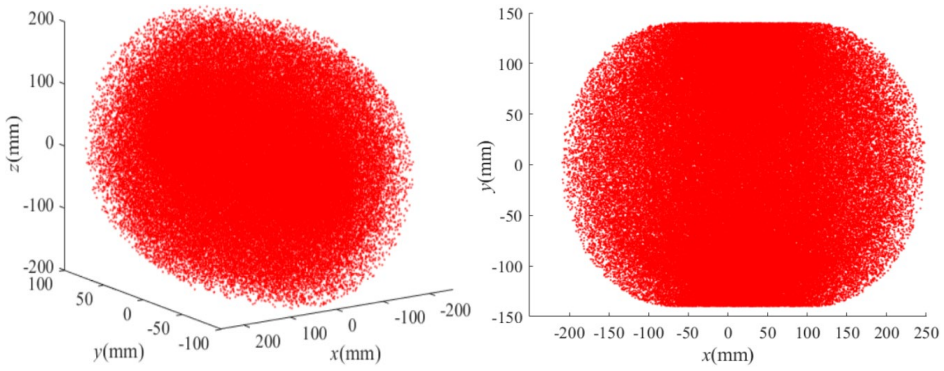

(a) *x-y-z* (b) *x-o-y*

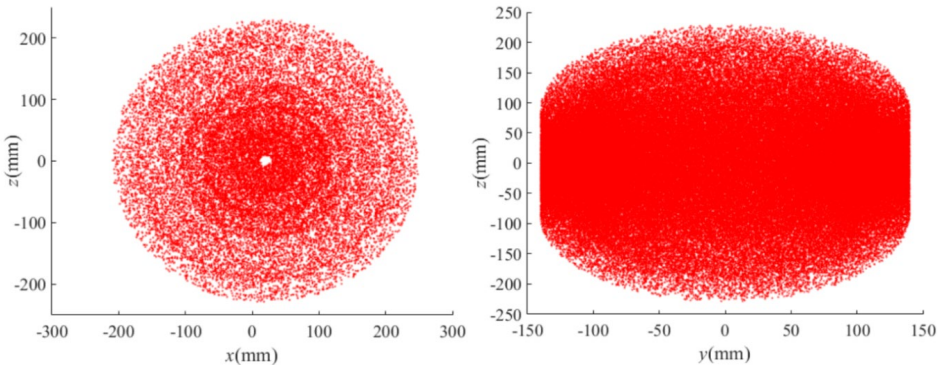

(c) *x-o-z* ($y \in [-25, 25]$mm) (d) *y-o-z*

Fig. 8. Contours of the 7-DOF manipulator workspace corresponding to group 1 of connecting rod

The workspace corresponding to the dimensions of the second group of connecting rods is shown in Figure 9. The voids in the workspace are searched along the *x*, *y*, and *z* directions with a thickness of 10mm for each layer. It is found that the second group of connecting rods had a void with a diameter of about 80mm in the *x-o-y* plane and within $z \in [-32, 32]$mm, as shown in Figure 9 (b).

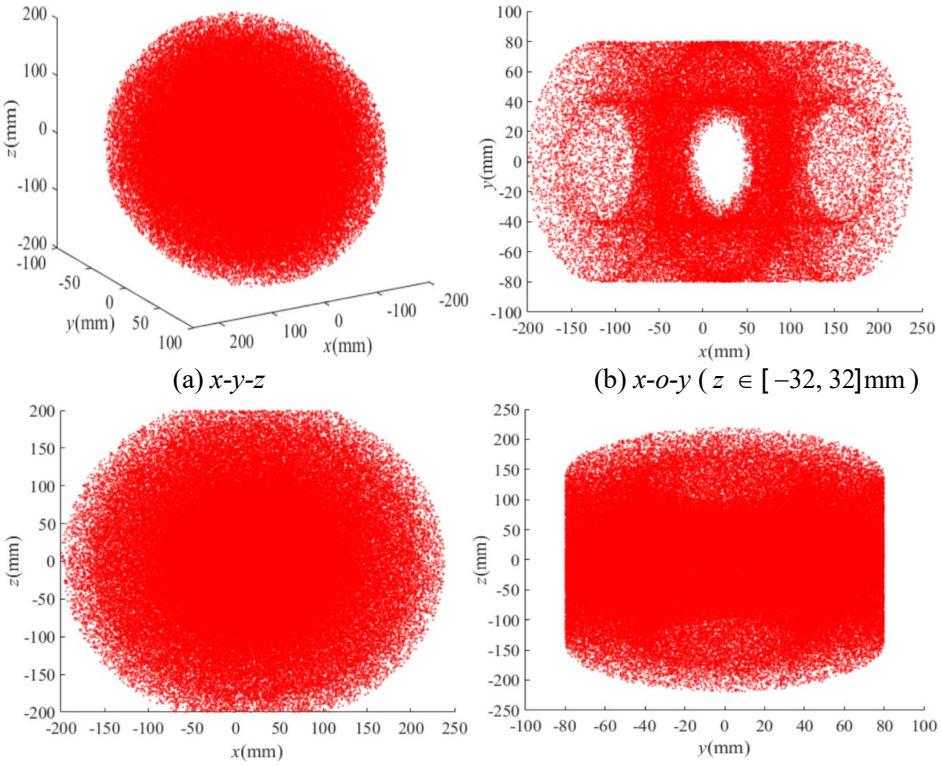

(a) *x-y-z* (b) *x-o-y* ($z \in [-32, 32]$mm)

(c) *x-o-z* (d) *y-o-z*

Fig. 9. Contours of the 7-DOF manipulator workspace corresponding to group 2 of connecting rod

The workspace corresponding to the dimensions of the second group of connecting rods is shown in Figure 10. The voids in the workspace are searched

along the *x*, *y*, and *z* directions with a thickness of 10mm for each layer. No voids are found. Although this method can determine whether there are voids in the workspace, the search method is inefficient and lacks reliability. By using the proposed workspace volume algorithm, the corresponding volume values for the three sets of connecting rod sizes are obtained as $V_1 = 4.2 \times 10^7\,\mathrm{mm}^3$, $V_2 = 3.8 \times 10^7\,\mathrm{mm}^3$, and $V_3 = 4.6 \times 10^7\,\mathrm{mm}^3$. Combining the volume of the manipulator workspace calculated in Section 2.2 and comparing the volume values of the workspace corresponding to the dimensions of the three groups of connecting rods, it can be found that the volume values of the third group change slightly, but the volume values of the first and second groups decrease significantly, indicating the presence of voids in these two groups of workspaces. Therefore, it can be concluded that the derived manipulator workspace no void constraint condition is effective.

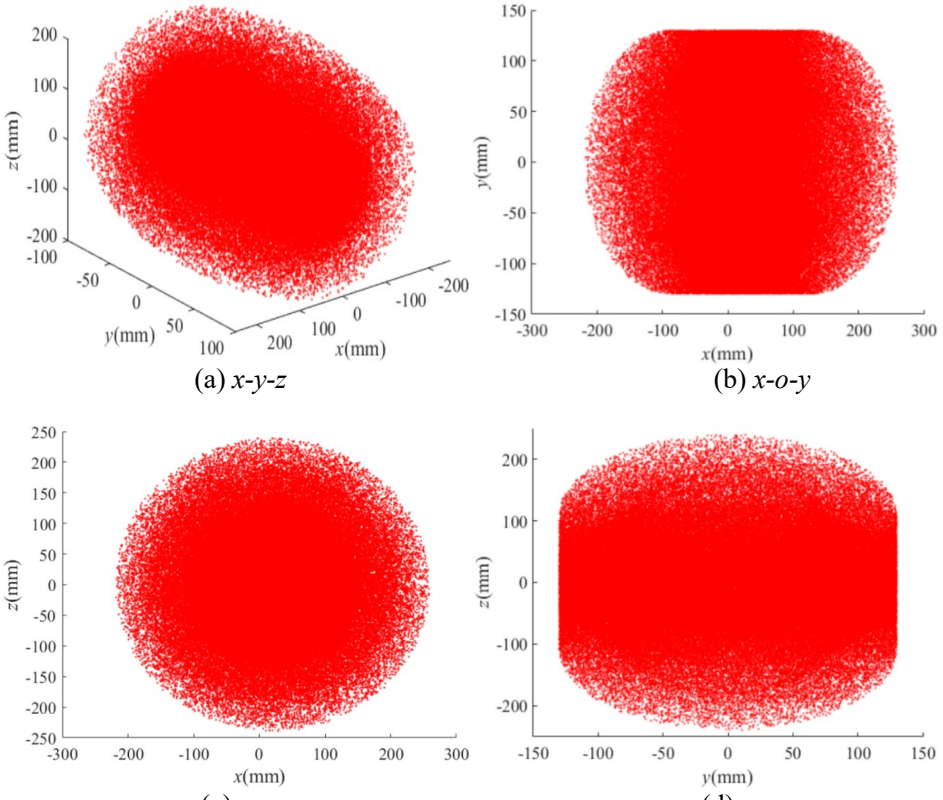

Fig. 10. Contours of the 7-DOF manipulator workspace corresponding to group 3 of connecting rod

5. Conclusions and future work

A 7-DOF manipulator workspace volume solving algorithm, based on the principle of three-dimensional function calculus, has been proposed. This algorithm addresses the difficulty of identifying changes in the workspace obtained by the Monte Carlo method, which is not conducive to the optimization of linkage parameters when the workspace is used as the objective function. Furthermore, based on the 7-DOF manipulator, the constraint condition for its workspace without voids has been derived. By comparing the degree of change in the volume values corresponding to the dimensions of the three sets of manipulator links obtained through the workspace volume algorithm, it is easy to determine whether there are voids in the workspace. This approach avoids the low efficiency and reliability issues associated with searching for voids in the workspace cloud map. Meanwhile, it also verifies the effectiveness of the no void constraint condition. This provides a mathematical foundation for the selection of constraints and objective functions when optimizing the link parameters of the 7-DOF manipulator in the later stages.

In the future, we plan to use the no void workspace of the 7-DOF manipulator derived in this paper as one of the constraints, and the proposed workspace volume algorithm as one of the objective functions, to carry out multi-objective optimization analysis of the link parameters. Further, we will analyze the kinematics, trajectory planning, dynamics, and other characteristics of the optimized 7-DOF manipulator.

Acknowledgments

This work was supported by the Haizhou Bay Talent Innovation Fund of Jiangsu Ocean University (under Project No. KQ24024).

R E F E R E N C E S

[1]. *Q. Y. Zhang, Y. Zhang, H. R. Chen, H*. “Workspace and singularity analysis of desktop 607 manipulator”, Agricultural Equipment and Vehicle Engineering, **vol. 60**, no. 9, Sep. 2022, pp. 37-42.

[2]. *W. N. Hu*. “Optimization of arm length parameters for PUMA robots based on workspace”, Robot Technique and Application, **vol. 200**, no. 2021, Feb. 2021, pp. 23-27.

[3]. *T. M. Chen, Z. L. Yao, J. Zhang*. “The workspace computation of aerial platform truck based on Monte Carlo method”, Construction Machinery, **vol. 2**, no. 528, Jul. 2020, pp. 57-61.

[4]. *Q. Meng, Z. Jiao, H. Yu*. “Design and evaluation of a novel upper limb rehabilitation robot with space training based on an end-effector”, Mechanical Sciences, **vol. 12**, no. 1, May. 2021, pp. 639-648.

[5]. *R. T. Dou, S. B. Yu, F. Sun.* “Density-Reducing Monte Carlo Method for 7 Degrees of Freedom Humanoid Robot Arm Workspace Solution”, Journal of Southwest Jiaotong University, **vol. 58**, no. 06, Dec. 2023, pp. 1328-1338.

[6]. *Z. Y. Zhao, Z. B. Xu, J. P. He*. "Configuration Optimization of Nine Degree of Freedom Super-redundant Serial Manipulator Based on Workspace Analysis", Journal of Mechanical Engineering, **vol. 55**, no. 21, Nov. 2019, pp. 51-63.

[7]. *S. R. Pundru.* "Workspace Analysis of Calibrated Multi-position Synthesized 3-Prismatic-Revolute-Spherical Manipulator", Journal of the Institution of Engineers (India), Series C, **vol. 105**, no. 01, Jan. 2024, pp. 195-214.

[8]. *A. Peidro, R. Oscar, A. Gil, J. M. Marin, L. Paya*. "An improved Monte Carlo method based on gaussian growth to calculate the workspace of robots", Engineering Applications of Artificial Intelligence, **vol. 64**, no. 9, Nov. 2017, pp. 197-207.

[9]. *Z. Z. Liu, H. Y. Liu, Z. Luo.* "Improvement of Monte Carlo method for solving robot workspaces", Transactions of the Chinese Society for Agricultural Machinery, **vol. 44**, no. 1, Jan. 2013, pp. 230-235.

[10]. *Z. B. Xu, Z. Y. Zhao, S. He.* "Improvement of Monte Carlo method for robot workspace solution and volume calculation", Optics and Precision Engineering, **vol. 26**, no. 11, Dec. 2018, pp. 2703-2713.

[11]. *H. B. Liu, D. X. Geng, G. B Wu*. "Research on forward kinematics of mechanical arm and workspace of its end robot hand", Machine Tool and Hydraulics Mach Tool Hydrau, **vol. 50**, no. 03, Mar. 2022, pp. 15-20.

[12]. *Z. H. Lan, M. W. Su*. "Analysis of the Flexible Workspace and Its Void of the Planar Parallel Manipulator", Proceedings of the 12th National Symposium on Mechanism and Machine Science, **vol.3**, Dec. 2000, pp.128-129.